Forest Ecology and Management 451 (2019) 117490

Contents lists available at ScienceDirect

Forest Ecology and Management

journal homepage: www.elsevier.com/locate/foreco

Burn probability simulation and subsequent wildland fire activity in Alberta, Canada – Implications for risk assessment and strategic planning

Jennifer L. Beverly[a,*], Neal McLoughlin[b]

[a] Department of Renewable Resources, University of Alberta, Edmonton, AB T6G 2H1, Canada
[b] Forestry Division, Alberta Agriculture and Forestry, 9th Floor, 9920 – 108 Street, Edmonton, Alberta T5K 2M4, Canada

ARTICLE INFO

Keywords:
Landscape simulation
Hazard
Risk
Burn probability
Wildfire
Burn-P3

ABSTRACT

Burn probability maps produced by Monte Carlo methods involve repeated simulations of fire ignition and spread across a study area landscape to identify locations that burn more frequently than others. These maps have achieved broad acceptance for research investigations and strategic fire management planning. In this study, we investigated correspondence between burn probability heat maps and burned areas observed in subsequent years for five study areas in Alberta, Canada. Observations of burned areas included 138 fires that collectively burned 543 049 ha. Distributions of burn probability values within burned areas were not heavily skewed towards the high-end of the range; however, median burn probability was significantly lower in unburned areas compared with burned areas for three of five study areas. Accuracy of burn probability maps was dependent on map design choices and subjective performance thresholds. When continuous burn probability values were mapped with a stretched symbology, most observed burned areas (> 70%) were located in areas within the lower-half of the burn probability range where fires were considered the least likely. In contrast, when burn probabilities were mapped and evaluated with a 50th percentile performance threshold, most observed burned areas (75–80%) occurred in half of the study area where burn probability values exceeded the median. Map accuracy declined linearly as this performance threshold was increased from 50th to 90th percentile. Choice of classification method for mapping burn probabilities altered the appearance of the map and corresponding map accuracy. Compared with Jenks natural breaks, equal intervals, or defined intervals, a quantile classification was the only method that resulted in burned areas falling preferentially in locations mapped in the highest burn probability classes.

1. Introduction

Burn probability maps generated by Monte Carlo simulation are widely used in research and fire management planning to identify areas of the landscape that are most likely to burn. The modeling process involves repeated trials during which initiation and spread of one or more fire ignitions is simulated to map burned areas across a study area during a given time period. Burn probability is typically assessed as the number of times a location burned in relation to the number of independent trials or model iterations. Burn probability values are displayed as a heat map that communicates relative spatial variation in the likelihood of burning. As an early proponent of the approach, Clarke et al. (1994) emphasized the value of burn probability maps for communicating fire hazard to the public, land developers and other stakeholders. The complexity and computational intensity of burn probability modeling was initially considered prohibitive for widespread use in management applications (Farris et al., 2000). Innovations in computing technologies over the past two decades have enabled increasing use of the approach, with many researchers extolling the significance and promise of burn probabilities from Monte Carlo simulations for quantifying wildland fire risk (i.e., Carmel et al., 2009; Keane et al., 2010; Weise et al., 2010; Parisien et al., 2013).

Recent burn probability maps generated from Monte Carlo simulations have been used to identify 'hot spots' and 'cold spots' of fire likelihood across diverse study areas located in Spain (Alcasena et al., 2017), China (Ye et al., 2017), Korea (Woo et al., 2017), the United States (Lautenberger, 2017), Canada (Wang et al., 2016), and Greece (Mallinis et al., 2016). Burn probability models have also been applied in large-scale risk assessments across expansive areas, for example Finney et al. (2011) used the FSim simulation system to map burn probabilities across the contiguous land area of the United States.

Baseline burn probability maps representative of current conditions

* Corresponding author.
E-mail address: jen.beverly@ualberta.ca (J.L. Beverly).

https://doi.org/10.1016/j.foreco.2019.117490
Received 9 May 2019; Received in revised form 16 July 2019; Accepted 19 July 2019
Available online 20 August 2019

within a study area are often compared with paired maps generated from modified model inputs to assess mitigation alternatives, such as fuel treatment scenarios (e.g., Beverly et al., 2009; Salis et al., 2016; Salis et al., 2018) or the effects of changing weather conditions indicated by climate change scenarios (e.g., Williamson et al., 2008; Wang et al., 2016; Lozano et al., 2017). Burn probability maps have also been used in research investigations of the effect of this type of 'science-based' risk evidence on decision making processes (e.g., Sherry et al., 2019). Widespread acceptance of burn probability maps has led to expanded use beyond direct fire management applications to inform broader land management issues such as species conservation efforts (e.g., Chiono et al., 2017; Whitman et al., 2017; Stockdale et al., 2019).

In addition to the growing popularity of burn probability simulation in varied research investigations, burn probability mapping has been embraced by fire management agencies for communicating risk and informing strategic planning processes. In the province of Alberta, Canada, the agency responsible for fire management began producing burn probability maps for strategic planning purposes in 2013 using the Burn-P3 model (Parisien et al., 2005), which was developed by a team of fire researchers at the Canadian Forest Service. Rapid adoption of burn probability simulation as an applied fire management decision support tool is consistent with broad developments in risk-based governance outlined by Nobert et al. (2015) in which anticipatory quantitative tools are deemed essential for defining and structuring future risks. Uptake of burn probability simulation models by management agencies seeking to demonstrate an evidenced-based approach to fire management planning has been expedited by freely available software like Burn-P3 and the ease with which these complex, computationally intensive models can be run using modern desktop computing technologies.

As burn probability maps gain influence and popularity for decision support, there is a need to apprise current and prospective users of their accuracy and limitations for informing management actions. Few studies have examined observed burned area in relation to pre-fire risk maps generated from Monte Carlo simulations. An exception can be found in Paz et al. (2011), which documented the area burned by a single large fire in Israel in relation to a pre-fire burn probability map produced from 1000 fire growth simulations using the FARSITE fire growth model (Finney, 2004). In this study we take a similar approach to evaluate correspondence between observed burned areas and pre-fire assessments of burn probability generated with the Burn-P3 simulation model for multiple study areas in Alberta, Canada.

Burn-P3 simulates fire processes nested within multiple spatial and temporal scales. Fire ignitions, fire spread, and fire regime characteristics such as the fire-size distribution are all modeled with inputs parameterized to produce results that conform to known fire activity documented for the area under consideration during the recent historical period. Model results are therefore dependent on the historical time period and choice of study area extent defined by the modeler. Resulting burn probability values are informative for the study area where they were generated and are used by decision makers as a relative rating of fire likelihood for that specific area.

Burn probability maps used in this study represent a range of spatial scales and were parameterized using a range of temporal scales. Accordingly, we assessed the accuracy of each burn probability map independently. All five burn probability maps were completed for study areas in the province of Alberta, Canada, and include a West Central (WC) Alberta research area (Beverly et al., 2009) and four maps produced by the Government of Alberta for individual fire management compartments: Lac La Biche (LLB), Fort McMurray (FTMC), Calgary (CLGY), and Willmore Wilderness (WW). We used the Government of Alberta's province-wide database of fire polygons representing historical fire perimeters to map burned areas in each of these five study areas in the years that followed burn probability simulations.

Following Paz et al. (2011) we considered burn probability maps effective if observed burned areas occurred predominantly in locations that were assessed as having a relatively high likelihood of burning prior to the fire (i.e., locations on the map displayed as hot spots). Our aim is to provide insight about the accuracy of burn probability maps for their intended applied use by practitioners for decision support. We investigate the extent to which burn probability maps generated with standard modeling software following published procedures and recommendations for model settings and parameters were effective for their intended purpose over the time frame these maps were considered useful for decision support. Expectations of decision makers who use burn probability maps to inform their actions are therefore central to our investigation.

Burn probability values are typically displayed for decision makers as a heat map with a classification scheme that sets and defines colors associated with specific ranges of values. Arbitrary map design decisions can potentially introduce errors and bias in interpreting data, as reviewed by Seipel and Lim (2017) in the context of flood hazard mapping. Map classification methods, number of bins (i.e., classes), and color selections published in previous burn probability studies vary widely. Beverly et al. (2009) smoothed raw burn probability values with a 500-m radius circular neighborhood to address deficiencies in the replicability of Burn-P3 results and displayed results using a natural breaks (Jenks) classification with 5 bins. Lautenberger (2017), Ye et al. (2017), and Stockdale et al. (2019) display burn probabilities with equal interval classes using 20, 10 and 6 bins, respectively. Woo et al. (2017) display burn probabilities across 10 bins, of which 9 are equal and the largest class includes values above a threshold. Mallinis et al. (2016), Salis et al. (2016, 2018) and Wang et al. (2016) all display burn probabilities with unequal-sized bins derived from unreported classification schemes.

To assess the influence of subjective map design choices on the interpretation of burn probability maps and our assessment of their effectiveness for informing applied decision support, we created five versions of the same burn probability map for each study area by varying map symbology. In each of our five study areas, correspondence between observed burned areas and pre-fire burn probability maps was assessed for a range of possible performance thresholds to explore how the expectations of decision makers influenced our assessment of map accuracy. Implications for communicating burn probability results, assessing wildland fire risk and strategic fire management planning are discussed.

2. Methods

2.1. Study areas

Collectively, our five study areas span approximately 15.5 million ha equivalent to 38% of the provincial Forest Protection Area in Alberta (Fig. 1, Table 1). Study area sizes range from 1.3 million ha (CLGY) to 6.1 million ha (FTMC). Two study areas (LLB and FTMC) fall predominantly within the Boreal Natural Region (Natural Regions Committee, 2006). Two study areas (CLGY and WW) fall predominantly within the Rocky Mountain Natural Region. Both Boreal and Foothills Natural Regions are represented in the WC study area.

Study area fire regime characteristics representative of current conditions (1990–2017, Table 2A) were compiled from historical fire records obtained from the agency responsible for fire management in the province, Alberta Agriculture and Forestry. Annual fire numbers and area burned varies by study area with as few as 3 fires and < 1 ha burned during low activity years and over 400 fires and 650 000 ha burned during extreme years in which single fires have reached sizes exceeding 100 000 ha in three study areas (WC, LLB, FTMC). Concentration of large burned areas within a small number of years with notable large fires is characteristic of all five study areas. Examples are the 2016 Horse River Fire, also known as the "Fort McMurray Fire" (FTMC), the 2002 House River Fire (LLB), the 2002 Virginia Hills Fire (WC), the 2003 Lost Creek Fire (CLGY), and the 2006 Fetherstonhaugh

Fig. 1. Study area locations within the province of Alberta, Canada: WC –West Central study area of Beverly et al. (2009); LLB – Lac La Biche Forest Area; FTMC – Fort McMurray Forest Area; CLGY – Calgary Forest Area; and WW –Willmore Wilderness study area.

and Jackpine Fires (WW) which accounted for 27%, 40%, 53%, 52%, and 55% of area burned in their respective study areas between 1990 and 2017.

There are notable similarities between WC and LLB study areas with respect to number of fires per year, proportion burned annually, fire sizes, and proportion of lightning versus human caused fires. Ignition mechanisms differ between the FTMC study area, where almost all fires (79%) are caused by lightning and the CLGY study area where humans cause 93% of fires. Human ignitions in the CLGY study area result in relatively smaller fire sizes and annual burned areas in comparison with the other four study areas.

2.2. Burn probability simulation

Burn probability was assessed in all five study areas using the Burn-P3 model (Parisien et al., 2005), which is a publicly available software tool. Burn-P3 enables repeated, batch fire growth simulations across an area. A deterministic fire growth submodel, Prometheus (Tymstra et al., 2010) is used to grow each fire using spatial input data describing topography (slope, aspect, and elevation) and landcover type to predict

Table 1
Descriptions of the five study areas.

	Study Area				
	WC	LLB	FTMC	CLGY	WW
Study area extent[1] (ha)	2 378 217	4 026 647	6 078 433	1 264 914	1 717 265
Burnable area[2] (ha)	2 164 596	3 609 612	5 440 021	1 058 980	1 421 623
Natural Region[3]					
Foothills	68%	-	-	11%	36%
Boreal	32%	100%	85%	-	-
Rocky Mountain	-	-	-	86%	64%
Parkland	-	-		3%	
Natural Subregion(s)[4]	LF, UF, DM	DM, CM, LBH	NM,CM, LBH, UBH, KU, PAD, AP	A, SA, M, UF, FF, FP	A, SA, M, UF, LF
Dominant tree species[5] (ordered alphabetically)	Aw, Pl, Pb, Sw	Aw, Pb, Pl, Pj, Sb, Sw	Aw, Bw, Sb, Sw, Pb, Pj, Pl	Aw, Fa, Fd, La, Pl, Se, Sw	Aw, Fa, Fd, Pl, Pj, Se, Sb, Sw,
Elevations (meters ASL)	350–1350	387–941	169–868	1126–3278	786–3270

[1] Calculated as the count of pixels (each 100 m × 100 m in size) in the study area land cover grid used to derive Burn-P3 inputs.
[2] Study area extent excluding water and non-fuel land cover types. Equivalent to the count of pixels (each 100 m × 100 m in size) for which burn probabilities were estimated.
[3] Natural Regions < 1% of the study area omitted.
[4] Natural Subregion abbreviations: A = Alpine; AP = Athabasca Plain; CM = Central Mixedwood; FF = Foothills Fescue; FP = Foothills Parkland; KU = Kazan Uplands; LBH = Lower Boreal Highlands; LF = Lower Foothills; M = Montane; NM = Northern Mixedwood; PAD = Peace-Athabasca Delta; SA = Subalpine; UBH = Upper Boreal Highlands; UF = Upper Foothills.
[5] Tree species abbreviations: Aw = trembling aspen (*Populus tremuloides*); Bw = white birch (*Betula papyrifera*); Fa = alpine fir (*Abies lasiocarpa*); Fd = Douglas fir (*Pseudotsuga menziesii*); La = alpine larch (*Larix layallii*); Pj = Jack pine (*Pinus banksiana*); Pb = balsam poplar (*Populus balsamifera*); Pl = lodgepole pine (*Pinus contorta v. latifolia*); Sb = black spruce (*Picea mariana*); Se = Engelmann spruce (*Picea engelmannii*); Sw = white spruce (*Picea glauca*).

Table 2A
Current fire regime characteristics by study area 1990–2017.

	Study Area				
	WC	LLB	FTMC	CLGY	WW
Number of fires per year					
range	20–254	23–285	38–227	14–408	3–74
average	108	157	114	159	19
Area burned per year (ha)					
range	17–258 229	36–244 267	43–651 948	7–21 415	0.5–21 449
average	11 015	21 084	74 915	1353	1362
median	356	1161	9718	64	6
Average proportion burned per year[1]	0.005	0.006	0.014	0.001	0.001
Fire size (ha)					
range	0.01–163 138	0.01–238 867	0.01–577 647	0.01–18 966	0.01–14 554
average	102	134	659	9	70
Proportion of fires ≥1 ha	0.145	0.228	0.262	0.056	0.090
Proportion of area burned by fires ≥1 ha	0.999	0.999	> 0.999	0.995	0.999
Proportion of fires ≥10 ha	0.056	0.072	0.097	0.010	0.037
Proportion of area burned by fires ≥10 ha	0.996	0.996	0.999	0.980	0.996
Proportion of fires by cause lightning/human	0.45/0.55	0.40/0.60	0.79/0.21	0.07/0.93	0.62/0.38

[1] Proportion of the burnable area from Table 1.

fire spread as a function of fire weather using equations from the Canadian Forest Fire Behavior Prediction (FBP) System (Forestry Canada Fire Danger Group, 1992) and fire weather components of the Canadian Forest Fire Weather Index (FWI) System (Van Wagner, 1987). Fire numbers and sizes simulated by Burn-P3 during a model iteration reflect current conditions and are constrained by user-defined fire regime and fire environment attributes that are input into the model.

Burn probability maps for all of our study areas were generated using published procedures for modeling with Burn-P3. Historical fire and weather records were used to calibrate fire growth model inputs and other model parameters to ensure simulations produced fires with size distributions, numbers and ignition patterns consistent with recently observed fires. This calibration process validates that Burn-P3 is generating fires representative of real world fire activity. The duration of the historical baseline period used to parameterize and validate the model was 28 years in the WC study area and 53 to 54 years in the other four study areas. Fire regime characteristics for these varying baseline time periods are summarized in Table 2B.

For detailed documentation of the Burn-P3 model, refer to Parisien et al. (2005). Beverly et al. (2009) provide a succinct description of Burn-P3 modeling steps. Core Burn-P3 modeling processes do not vary from user to user and were consistent for all five of our study areas. Some simulation settings are adjusted by the modeler to suit their study area context, for example burn probability maps for our predominantly Rocky Mountain study areas (CLGY and WW) were generated using a modified approach to wind speed and direction described by Parisien et al. (2013) for use in landscapes with steep environmental gradients. The alternative statistical modeling approach for distributing lightning ignitions described in that study was not used due to a lack of statistical significance but was adopted for distributing human-caused fires in four of the study areas (LLB, FTMC, CLGY, WW). For ease of reference, key model settings and parameters for each of the five study areas are summarized in Table 3.

As noted in Beverly et al. (2009), Burn-P3 is designed to model 'escaped fires' that are considered large relative to the population of fires that occurred during the baseline historical period used to parameterize the model. The threshold size for defining an escaped fire in Burn-P3 was ≥4 ha, with the exception of the WC study area where a threshold of ≥10 ha was used. In our study areas, fires ≥10 ha are responsible for 98% to 99.9% of area burned (Table 2A, B) and fires < 10 ha in size can be considered inconsequential with respect to burned area.

Following each model iteration, Burn-P3 resets burned areas to an unburned state and the process is repeated until the desired number of iterations is reached. Burn probability is calculated for each pixel in the land cover grid as the number of times the pixel burned in relation to

Table 2B
Fire regime characteristics by study area for the baseline time periods used to calibrate burn probability simulations.

	Study Area				
	WC (1976–2003)	LLB (1961–2013)	FTMC (1961–2014)	CLGY (1961–2014)	WW (1961–2013)
Number of fires per year					
range	20–254	23–285	38–227	14–408	3–74
average	111	160	112	149	20
Area burned per year (ha)					
range	49– 229 995	36–244 267	43–651 948	7–21 415	0.5–21 449
average	11 191	21 964	58 479	1443	1066
median	383	1456	6447	62	54
Average proportion burned per year[1]	0.005	0.006	0.011	0.001	0.001
Fire size (ha)					
range	0.01–168 863	0.01–238 867	0.01–577 647	0.01–18 966	0.01–14 554
average	95	137	523	10	54
Proportion of fires ≥1 ha	0.195	0.234	0.268	0.061	0.078
Proportion of area burned by fires ≥1 ha	0.999	0.999	> 0.999	0.996	0.998
Proportion of fires ≥10 ha	0.057	0.074	0.093	0.011	0.034
Proportion of area burned by fires ≥10 ha	0.996	0.996	0.999	0.981	0.996
Proportion of fires by cause lightning/human	0.54/0.46	0.43/0.57	0.81/0.19	0.07/0.93	0.62/0.38

[1] Proportion of the burnable area from Table 1.

Table 3
Key specifications of burn probability simulations, by study area (WC, LLB, FTMC, CLGY, WW).

	Study Area				
	WC	LLB	FTMC	CLGY	WW
Baseline[1]	1976–2003 (28 years)	1961–2013 (53 years)	1961–2014 (54 years)	1961–2014 (54 years)	1961–2013 (53 years)
Reference year[2]	2005	2014	2016	2016	2014
Study area buffer[3] (km)	10	20	20	20	20
Iterations	25 000	34 200	2500	100 000	30 000
Simulated fires[4]	149 757	305 771	74 293	277 019	153 175

[1] Duration of baseline period used to parameterize model inputs from historical fire and weather data.
[2] Year representing the current condition of model inputs at the time the Burn-P3 simulation was completed.
[3] Used to minimize the impact of study area boundaries on simulated fire growth.
[4] Combined count of all modeled fires that were simulated during all Burn-P3 model iterations.

Table 4
Summary of post-simulation fire activity, by study area (WC, LLB, FTMC, CLGY, WW).

	Study Area				
	WC	LLB	FTMC	CLGY	WW
Post-simulation observation period (years)	2005–2017 (13)	2014–2017 (4)	2016–2017 (2)	2016–2017 (2)	2014–2017 (4)
Number of observed fires	53	48	23	7	7
Observed burned area[1] (ha)	33 671	91 238	406 683	1650	9807
Observation year-equivalents based on average annual area burned (1990–2017, Table 2)	3.1	4.3	5.4	1.2	7.2

[1]Calculated as the count of pixels (each 100 m × 100 m in size) in the burnable area from Table 1 that were burned by fires during the post-simulation observation period.
[2]Average burned area per year as a proportion of area available to burn from Table 1.

the number of opportunities it had to burn (i.e., number of iterations). As noted in Parisien et al. (2005), model results are considered representative of the likelihood of burning in a single year (i.e., over the next fire season) under current fire environment and fire regime conditions. The rate of departure from those current conditions with the passage of time will determine the duration over which model results apply. In all five of our study areas, fire regime characteristics estimated for current conditions (Table 2A, 1990-2017) are consistent with those estimated for the baseline period used for Burn-P3 simulations (Table 2B).

2.3. Post-simulation fire observations

We observed burned areas during time periods that began with the reference year for which simulation model inputs and settings were defined (refer to Table 3) and all subsequent years up to and including 2017. Burn probability was assessed at different points in the past, resulting in post-simulation observation periods that varied by study area from 2 to 13 years. Perimeters of fires that occurred in each study area during the observation period were compiled from a database of wildfire polygons obtained from the agency responsible for fire management in the province, Alberta Agriculture and Forestry.

The appropriate observation period and spatial extent of burned areas for assessing the performance of burn probability maps are interrelated factors that merit careful consideration. We considered an appropriate observation period to be one that was consistent in length with the intended timeframe over which these burn probability maps are considered useful for decision support. Burn-P3 produces a heat map displaying relative spatial variations in the likelihood of burning in a single year (i.e., over the next fire season) based on fire regime inputs that represent current conditions. Simulated burn probability maps could never be replicated in the real world by observing real fires. Validation of the modeling process is therefore limited to comparing simulated fires to those observed during the historical baseline period used to parameterize the model. Resulting burn probability maps are the combined result of thousands of possible fire seasons generated for a single point in time and the model does not incorporate landscape succession and change that would be necessary for simulating fire processes over longer time periods.

Due to infrequent large fires characteristic of our study areas, these ecosystems can experience substantial land cover change over short time periods that would quickly erode the representativeness of burn probability maps. Accordingly, our post-simulation fire observations were taken during a limited timeframe over which the burn probability maps are considered useful for decision support. Inter-annual variability in fire activity could result in these relatively short observation windows (i.e., 2–13 years) capturing only very minimal burned areas. Spatial extent of our observed burned areas was considered acceptable if it exceeded by multiple orders of magnitude the mean and median annual burned areas in our study areas over the recent historical period (1990–2017, Table 2A).

Fire observations included all mapped fires that burned areas equal to or greater than the minimum fire size used in Burn-P3 simulations which was 4 ha in all study areas excepting WC where a 10 ha minimum was used. We do not expect differences in minimum fire sizes used in simulations and observations to affect our results given the extremely small areas that fires < 10 ha contribute to area burned in our study areas (Table 2A,Table 2B).

To assess the influence of subjective map design choices on the interpretation and accuracy of burn probability maps, we generated five versions of the same burn probability map for each study area by varying map symbology. We used a ‘stretched’ symbology to display burn probability values from lowest to highest with a continuous color ramp. A series of four alternate maps was produced by applying common classification methods (quantile, Jenks natural breaks, equal interval, and defined intervals). Jenks natural breaks is a standard classification option automated in mapping software that optimizes class ranges to minimize the variance within classes and maximize the variance between classes (Jenks, 1967).

Burn probability maps are typically displayed using classes, rather than a stretched symbology, because classes help decision makers relate a discrete colour on the map to a specific burn probability range (e.g, 0.024–0.032) or qualitative meaning (e.g., “high”) that is communicated with the map legend. In comparison with a stretched symbology

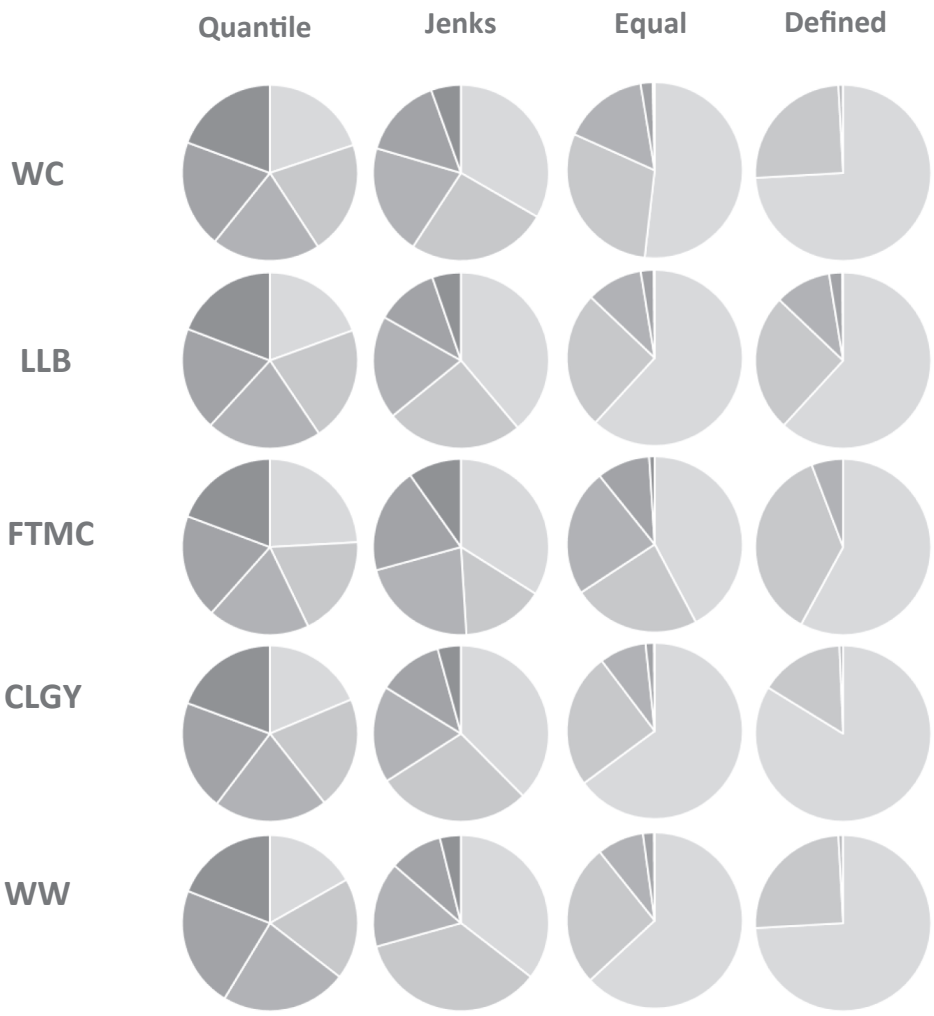

Fig. 2. Proportion of each study area (WC, LLB, FTMC, CLGY, WW) associated with a given burn probability class (light gray = low, dark gray = high), by classification method: quantile, Jenks natural breaks, equal interval, and a defined interval classification with percentile breaks at 34, 68, 95, 99 and 100. Refer to the Appendix for class break point values.

of continuous burn probability values, classes (bins) reduce spatial precision. Precision, or the spatial extent associated with a range of values, declines as bin numbers are reduced to the minimum possible in which a binary map is displayed with just two burn probability zones. In the case of an equal interval classification method, an extremely large number of bins will approximate the appearance of continuous values plotted with a stretched symbology. We chose a bin number representing the lower-bound of precision observed in our review of burn probability simulation studies (i.e., five), making it a conservative choice for evaluating map performance or accuracy. In the case of our defined interval classification we used unequal breaks at 34, 68, 95, 99, and 100 percentile, which correspond to classes used by the Alberta Government to map burn probabilities for strategic planning purposes.

As noted by Paz et al. (2011), if burn probability maps have no discriminatory power and the maps are not informative then burn probabilities within observed burned areas will not differ from the study area as a whole (i.e., the null model) and we would expect no differences in the distributions of burn probability values in burned and unburned areas. Proportions of burn probability values within burned areas were compared with null model proportions with Chi squared tests. Distributions of burn probability values in burned and unburned areas were compared with a Wilcoxon rank sum test. Due to the presence of spatial autocorrelation in the data, we used a random sample of burn probabilities consisting of a 0.005 portion of the area under assessment to test for significant differences, with the exception of CLGY burned area where a 0.015 proportion was sampled to ensure sufficient numbers. Differences in cumulative probability distributions of burn probability values in burned and unburned areas were assessed graphically. A Kolmogorov-Smirnov test was not viable due to the precence of ties in the data. Statistically significant differences in burn probabilities between burned and unburned areas or between burned areas and the study area as a whole can indicate that burn probability maps have some predictive value, but these differences alone provide little insight into map performance or accuracy.

Accuracy is the extent to which the result (observed burned areas) corresponds to expectations about what the burn probability map communicates to a decision maker. Boisvert et al. (2005) note that when assessing the quality of a result in scientific computing, comparison with an external standard is required (i.e., the correct answer). The correct answer for a burn probability map will depend on expectations. An expectation that the majority of burned areas will occur in half of a study area where burn probability values exceed the median corresponds to a 50th percentile performance threshold. Paz et al. (2011) used a 70th percentile performance threshold to evaluate the accuracy of a burn probability map, reporting that 87% of observed burned area occurred in locations with burn probability values in the top 30%. The spatial extent of these expectations describes the precision of the expected result. Quantile performance thresholds have a

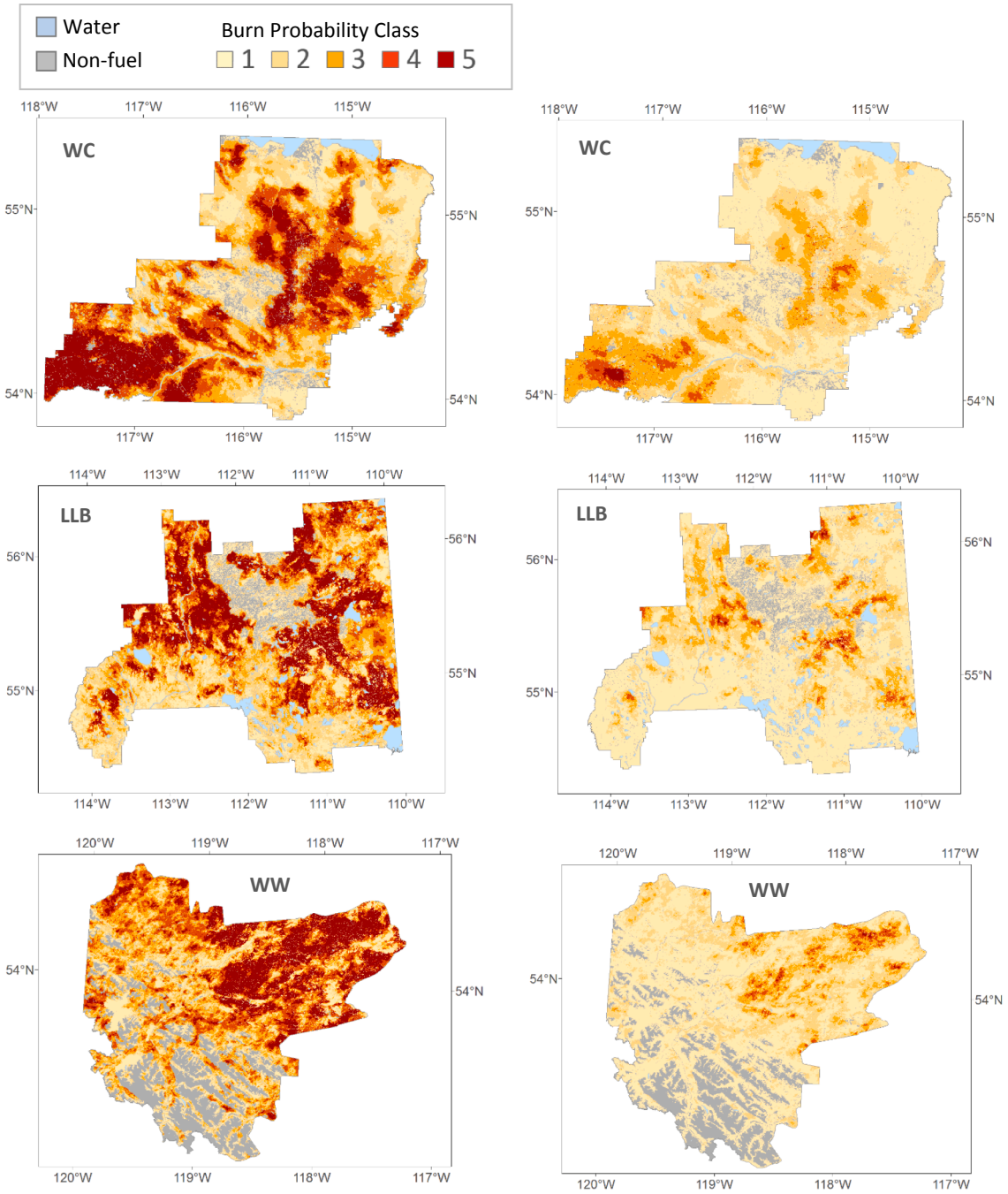

Fig. 3. Comparative burn probability maps by study area (WC, LLB, FTMC, CLGY, WW) for two classification methods: quantile (left) and equal interval (right). Refer to the Appendix for class break point values.

readily understood spatial precision: 30% of the study area has burn probabilities that exceed the 70th percentile. Alternate performance thresholds could be derived from the numerical range of burn probability values, such as an expectation that the majority of burned areas will occur in the upper-half of the range. In these cases, the corresponding spatial precision will depend on the distribution of burn probability values.

We compared multiple alternate performance thresholds for assessing the accuracy of burn probability maps simulated for our five study areas. For each study area we calculated the percent of observed burned area with burn probabilities exceeding performance thresholds ranging from the 50th to 90th percentile. We also measured map accuracy as the percent of observed burned area that had burn probabilities that exceeded the mid-value of the burn probability range. In all cases, we considered a score of 100% to indicate perfect map accuracy and a score $< 50\%$ to indicate poor performance for applied decision support.

3. Results

3.1. Post-simulation fire observations

Observed burned areas in all five study areas confirmed the extremely low likelihood that a given location will be burned by a fire over the short term in these ecosystems. The vast majority (92.5–99.8%) of each study area remained unburned in the years that

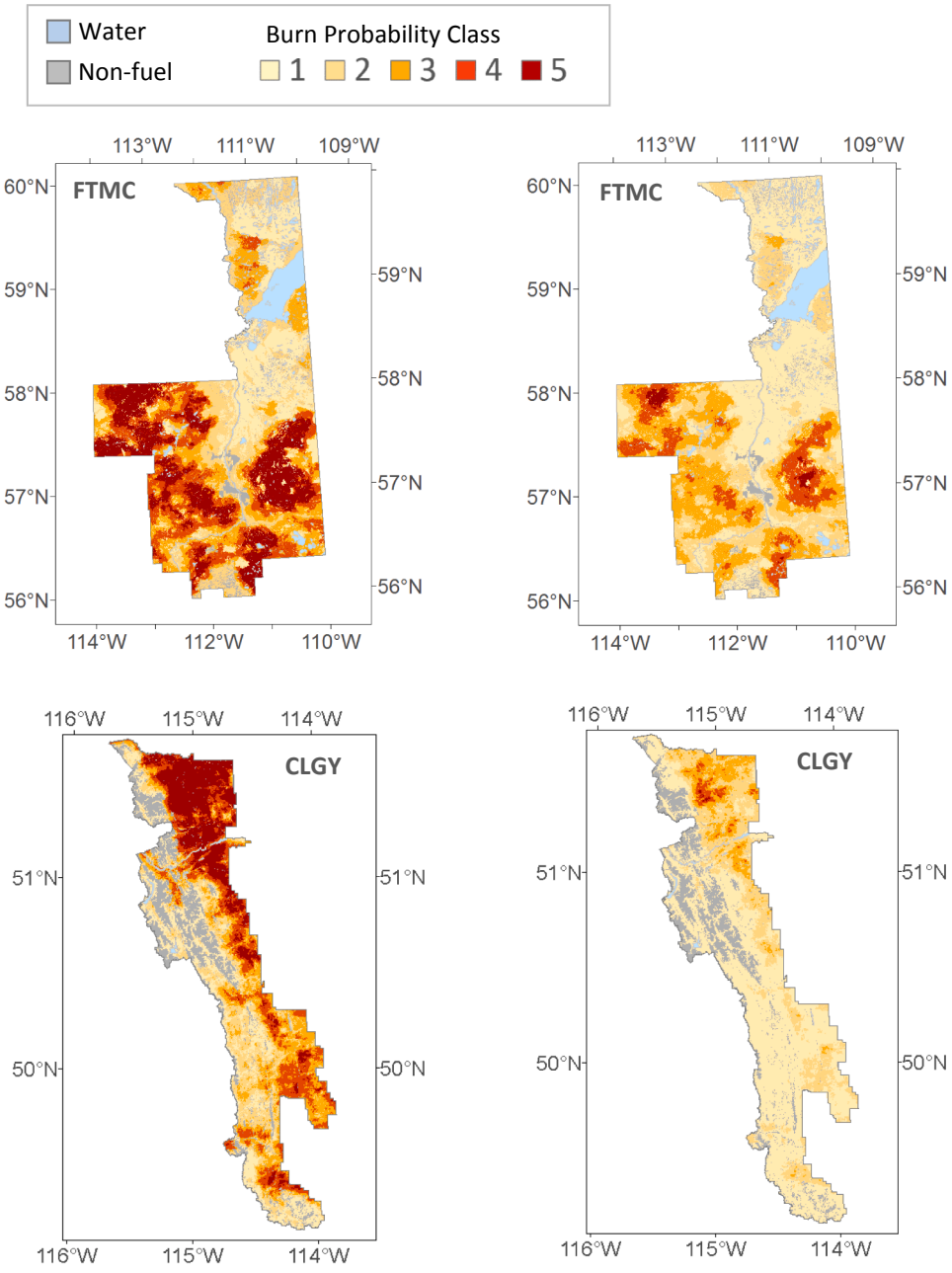

Fig. 3. (*continued*)

followed the burn probability assessment. Despite the low likelihood of burning in these landscapes, we observed 138 fires or portions of fires in the five study areas in the years that followed burn probability simulations. Collectively, these fires burned a total of 543 049 ha or an area more than half the size of Yellowstone National Park.

Fire observations by study area are summarized in Table 4. The extent of observed burned areas varied from 1650 ha in the CLGY study area to 406 683 in FTMC (Table 4). In comparison with average annual area burned over the recent historical period (1990–2017, Table 2A), observed burned areas had year-equivalents that ranged from 1.2 to 7.2 years. Observed burned areas were also 42–95 times greater than median annual burned area in our Boreal and Foothills study areas (WC, LLB, FTMC) and 26 to 1635 times greater in our Rocky Mountain study areas (CLGY and WW). All but one study area contained burned area observations that were multiple orders of magnitude greater than average and median annual burned areas, which suggests possible under-sampling of burned areas is limited to the CLGY study area.

3.2. Burn probability maps

Burn probability simulations indicated that the likelihood of a location being burned by a fire over the next fire season is extremely low across all five study areas (Table 4). Maximum burn probabilities ranged from 0.0018 to 0.0616, which corresponds to a 93.8% to 99.8% chance that the assessed pixel will remain in an unburned state over the next fire season. Mean and median burn probabilities were highest in the WC and FTMC study areas and notably lower in the LLB, CLGY and WW study areas.

As expected, continuous burn probability values displayed with a stretched symbology (not shown) approximated the appearance of values mapped with an equal interval classification and we therefore focused our comparisons of map symbologies on the four alternate classification methods. When burn probability values were classified into five bins, the proportion of the study area associated with a given class varied depending on the choice of classification method (Fig. 2).

Table 5
Summary statistics of burn probability values in burned and unburned areas by study area (WC, LLB, FTMC, CLGY, WW) for two extents: (A) all land; and (B) a random sample covering 0.005 of the area excepting CLGY burned area where a 0.015 proportion was sampled. Due to the presence of spatial autocorrelation in the data, tests for significant differences apply only to sampled locations.

(A) All land areas

		Area[a]	Range	Median	Mean	SD
WC	Unburned	2 130 925	0–0.0078	0.0015	0.0018	0.0014
	Burned	33 671	0–0.0053	0.0022	0.0022	0.0010
LLB	Unburned	3 518 374	0–0.0041	0.0005	0.0007	0.0007
	Burned	91 238	0–0.0033	0.0012	0.0013	0.0008
FTMC	Unburned	5 033 338	0–0.0616	0.0155	0.0166	0.0149
	Burned	406 683	0–0.0552	0.0242	0.0247	0.0099
CLGY	Unburned	1 057 330	0–0.0019	0.0003	0.0003	0.0003
	Burned	1650	0–0.0010	0.0002	0.0003	0.0001
WW	Unburned	1 410 816	0–0.0018	0.0003	0.0003	0.0003
	Burned	9807	0–0.0012	0.0002	0.0002	0.0002

(B) Sampled locations

		Area[a]	Range	Median	Mean	SD
WC	Unburned	9694	0–0.0077	0.0015	0.0018[b]	0.0014
	Burned	154	0–0.0047	0.0021	0.0022	0.0010
LLB	Unburned	16 974	0–0.0038	0.0005	0.0007[b]	0.0007
	Burned	426	0–0.0031	0.0013	0.0013	0.0008
FTMC	Unburned	24 019	0–0.0592	0.0156	0.0164[b]	0.0147
	Burned	1923	0–0.0484	0.0251	0.0253	0.0098
CLGY	Unburned	4835	0–0.0017	0.0003	0.0003	0.0003
	Burned	25	0–0.0004	0.0002	0.0002	0.0001
WW	Unburned	6571	0–0.0017	0.0004	0.0003	0.0003
	Burned	49	0–0.0008	0.0002	0.0002	0.0001

[a] Count of 100 m × 100 m pixels in the burnable area from Table 1.
[b] Significantly less in comparison with burned areas (Wilcoxon rank sum test, $p < 0.00001$).

Consequently, burn probability maps produced for the same study area using identical Burn-P3 results and color choices but different classification methods had dramatically different appearances (Fig. 3). Under a quantile classification, a large portion of the study area (i.e, 20%) is associated with the highest burn probability class and vast land areas (i.e., 205 001 ha to over one million hectares) appear relatively fire-prone. Equal interval classes result in a map with just 0.1% to 1% of the study area falling within the highest burn probability class, giving the impression that areas with the highest fire likelihood are comparatively limited in extent (1042–54 832 ha).

3.3. Observed burned areas and pre-fire burn probability

Median burn probabilities were significantly lower in unburned areas compared with burned areas in three of the five study areas (WC, LLB, FTMC – Table 5); however, in all study areas the magnitude of these differences was very small. In the WC study area, the median likelihood of an area remaining in a fire-free state over the short term was 99.85% in areas that did not burn and 99.78% in areas where fires occurred. In the LLB study area, median burn probabilities indicated the likelihood of remaining fire-free was 99.95% in unburned areas and 99.88% in locations where fires actually occurred.

If burn probability maps are effective at identifying locations that are most likely to burn in a given landscape, we would expect burned areas to contain burn probability values skewed towards the high-end of the range of burn probability values in the study area. Cumulative distribution functions (CDFs) shown in Fig. 4 revealed that large portions of burned areas in all five study areas were assessed as having relatively low burn probability values prior to the fires. The vast majority (72–100%) of observed burned areas had pre-fire burn probability values that were in the lower-half of the range of values within the study area as a whole. Consequently, a map of continuous burn probability values using a stretched symbology or a map with an equal interval classification of values would have the effect of communicating the opposite of what a decision maker would intuitively expect: almost all observed burned areas are located in areas identified by the lower-half of the color ramp (i.e., locations displayed as fire cold spots).

Distributions of burn probability values in burned areas were visibly different in comparison with distributions for the study area as a whole (i.e., null model proportions) (Fig. 5), but these differences varied by study area and classification method. When a quantile classification method was used, the expected pattern of disproportionately large burned areas falling within the highest burn probability classes was realized for three study areas (WC, LLB, FTMC). When an equal interval or defined interval classification method was used, burned areas did not occur disproportionately in locations assessed as having the highest burn probability class. For these classification methods, moderate to low burn probability classes had disproportionately higher burned areas for most study areas. For three study areas (WC, LLB, FTMC), burned areas also occurred disproportionately within moderate burn probability classes (i.e., classes 3 and 4) when Jenks natural breaks were used to classify the data. As expected, these results were not sensitive to the number of bins used to classify burn probabilities (Fig. 6 – WC example). Increasing bin numbers from five to ten added precision to mapped values but did not change the shape of the distributions or the pattern of disproportionate burned areas observed when five bins were used.

Proportions of observed burned areas with burn probability values exceeding a range of subjective performance thresholds are shown in Table 6. Burn probability maps for two study areas (CLGY and WW) exhibited poor accuracy irrespective of the percentile threshold. For WC, LLB, and FTMC study areas, burned area proportions were significantly different from the null model for most performance thresholds and map accuracy was very high when a relatively low quantile threshold was used (Fig. 7) with 75–82% of burned areas associated with burn probability values above the median (50th percentile). This performance threshold corresponds to a burn probability map displayed with just two classes that each cover one-half of the study area and an expectation that burned areas are most likely in the “high” half. In comparison, only 33–53% of burned areas had burn probabilities that exceeded the 75th percentile, which covered an area equal to one quarter of the study area and 21–44% of burned areas had burn probability values that exceeded the 80th percentile equivalent to one fifth of the study area. We considered map accuracy < 50% indicative of poor performance for applied decision support. Results for our study areas suggest that burn probability maps are effective when up to three quantile classes are used to map values and decision makers expect most burned areas to occur in the top third of the study area where burn probability values exceed the 67th percentile.

Burn probabilities mapped with high levels of spatial precision performed poorly. The linear negative relationship between map accuracy and spatial precision shown in Fig. 7 is remarkably consistent between WC and FTMC study areas. Burn probability maps for these two study areas were generated a decade apart by different modelers using different baseline calibration periods, different minimum fire sizes for simulations, different approaches for distributing human-caused fires, and different numbers of iterations. There were also marked differences between these two study areas with respect to study area size, duration of post-simulation fire observations, number of observed fires and the spatial extent of observed burned areas, yet the tradeoff between map accuracy and precision is virtually identical. In contrast, the LLB and FTMC burn probability maps were produced by the same modeler using the same settings, with the exception of iteration numbers, yet the LLB burn probability map exhibited consistently higher map accuracy compared with FTMC. Variation in the quality of data inputs between LLB and FTMC study areas may be a possible explanatory factor. Land cover data input for Burn-P3 simulations were considered substantially more accurate in the LLB study area compared with FTMC.

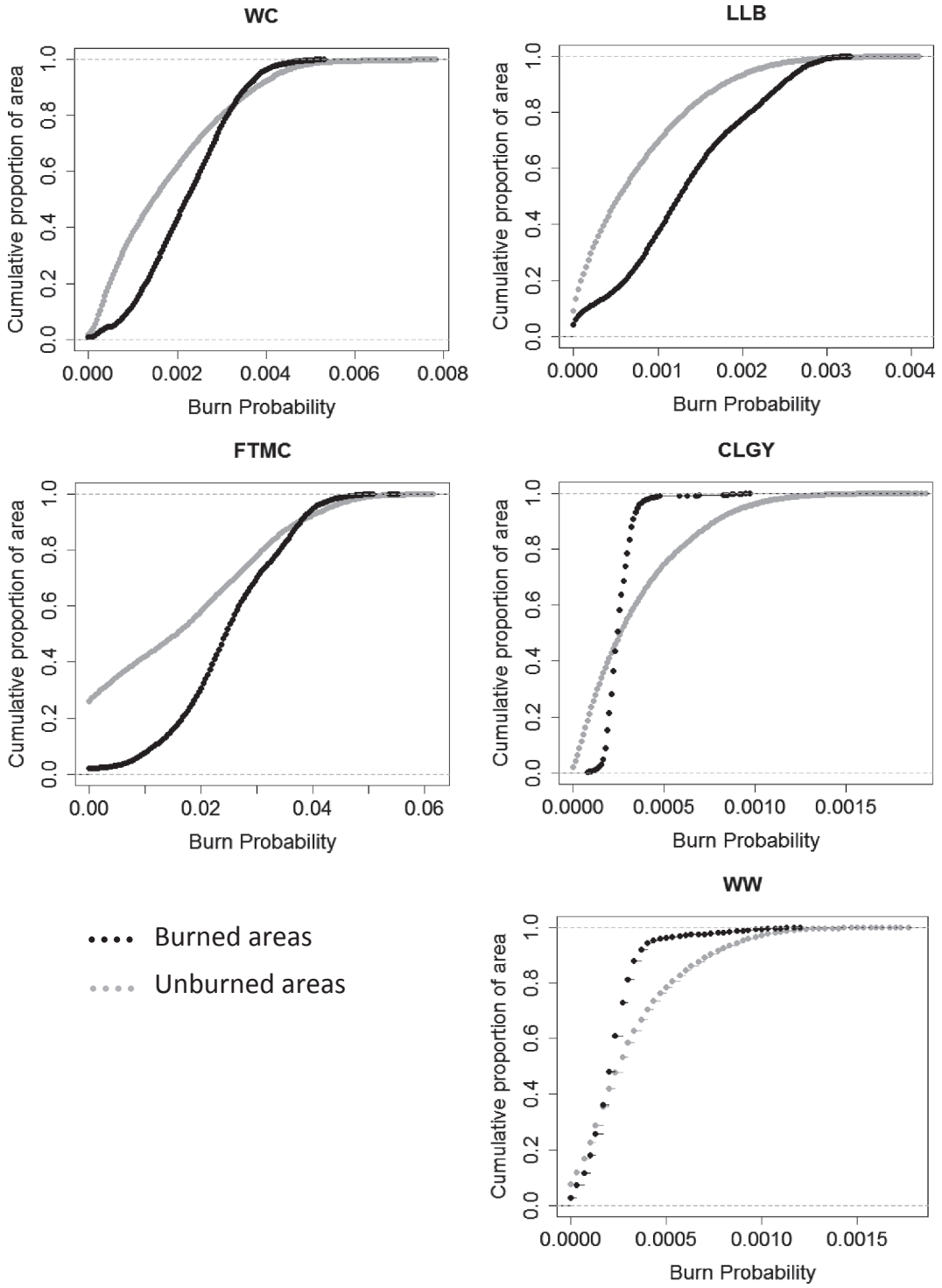

Fig. 4. Cumulative distribution functions of burn probability values in unburned (gray) and burned (black) areas, by study area (WC, LLB, FTMC, CLGY, WW).

Poor performance of the CLGY burn probability map may be the result of possible under-sampling of burned areas in that study area. Poor performance of burn probability maps for CLGY and WW study areas located predominantly in the Rocky Mountain Natural Region may be a general indication of the limitations of the Canadian Forest Fire Behavior Prediction (FBP) System models for simulating fire growth in the vegetation types and complex terrain characteristic of these areas. Conifer fuels typical of higher elevations (Table 1) such as alpine fir, Engelmann spruce, and alpine larch are not well represented by FBP System fuel types. In contrast, fuel types in the WC, LLB and FTMC study areas are well-represented by FBP System fuel types for dominant conifer forest stands, such as C-2 Boreal Spruce and C-3 Jack or lodgepole pine.

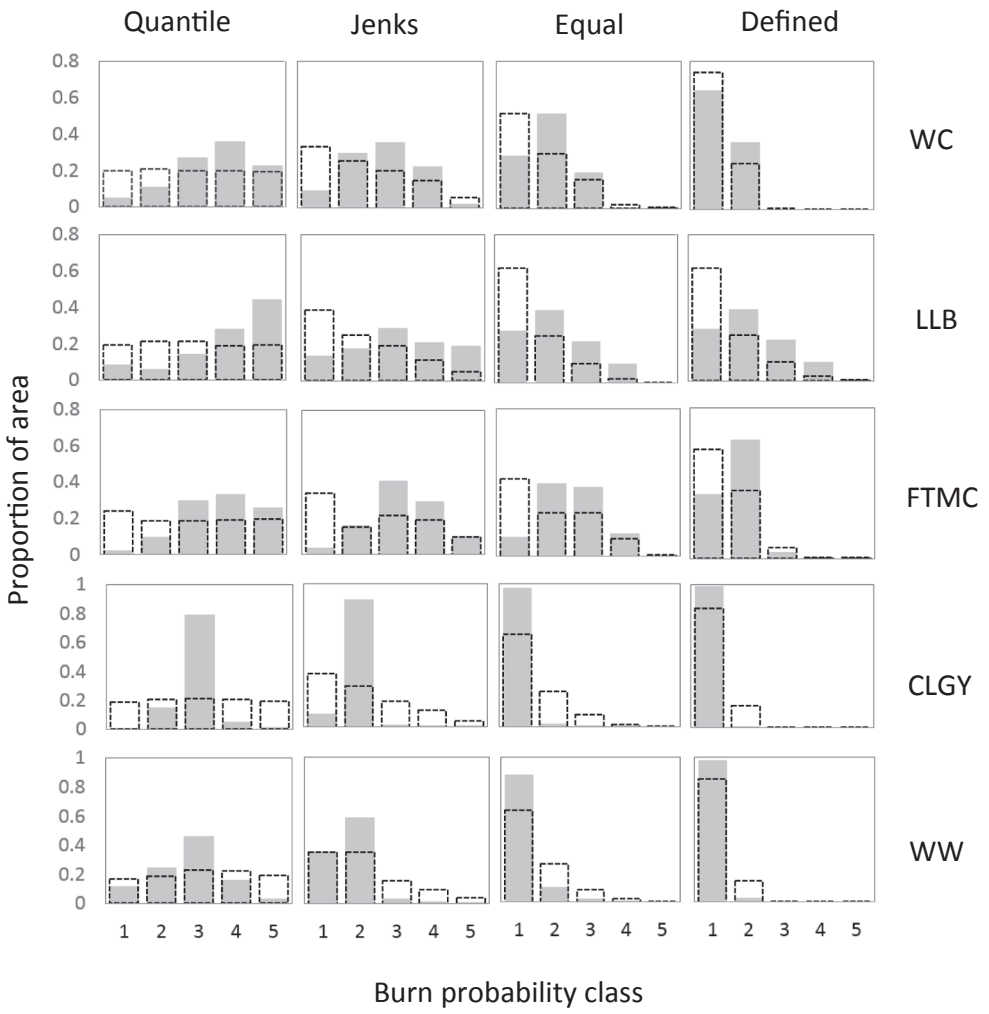

Fig. 5. Burned area proportions (solid shaded bars) versus study area null model proportions (hollow dashed bars) by burn probability class (1 = low, 5 = high) and study area (WC, LLB, FTMC, CLGY, WW) for four classification methods: quantile, Jenks natural breaks, equal interval and a defined interval classification with percentile breaks at 34, 68, 95, 99 and 100. Refer to the Appendix for class break point values.

4. Discussion

For two study areas located predominantly in the Rocky Mountain Natural Region of Alberta, burn probabilities in burned areas were not significantly different from those in unburned areas. Significant differences in burn probabilities between burned and unburned locations were found for three study areas located in Boreal and Foothills Natural Regions (WC, LLB, FTMC). In these study areas, median burn probabilities were all significantly lower in unburned areas compared with burned areas; however, in all five study areas, large portions of burned areas observed in the years following burn probability simulations occurred in locations where burn probabilities were relatively low.

Implications of these results depend on expectations about what burn probability maps communicate to decision makers and the nature of the decisions these maps are intended to inform. Previous studies have promoted simulated burn probability maps for fine scale applications, such as assessing susceptibility of burning around very localized features like communities, roads, pipelines or habitat areas (Parisien et al., 2013; Stockdale et al., 2019). Others have either used or promoted burn probability simulations as a tool for evaluating relatively fine-scale fuel management scenarios (e.g., Beverly et al., 2009; Finney et al., 2011; Salis et al., 2016, 2018; Chiono et al., 2017). Burn probability maps produced with Monte Carlo simulations have even been recommended for identifying areas of expected insurance losses (e.g., Alcasena et al., 2017). Developers of the Burn-P3 modeling software claim burn probability maps provide a high-resolution assessment of wildfire susceptibility across a study area that can be used to prioritize fire management efforts and identify optimal locations for look-out towers, fire control lines, firefighter safety zones and fuel treatment mitigation activities around communities (Parisien et al., 2005).

For three of our study areas where burn probability maps appeared to have some predictive potential (WC, LLB, FTMC), performance of the maps depended heavily on map design choices and subjective thresholds for assessing accuracy. Maps visualized with the highest possible spatial precision (i.e., continuous values displayed with a stretched symbology) performed very poorly with 72% to 100% of observed burned areas located in areas represented by the lower-half of the burn probability color ramp (i.e, the fire cold spots). When expectations for spatial precision were relaxed, the performance of burn probability maps improved: most observed burned areas (75–80%) in WC, LLB and FTMC study areas were located in the half of the study area where burn probability values exceeded the median. Unfortunately, a burn

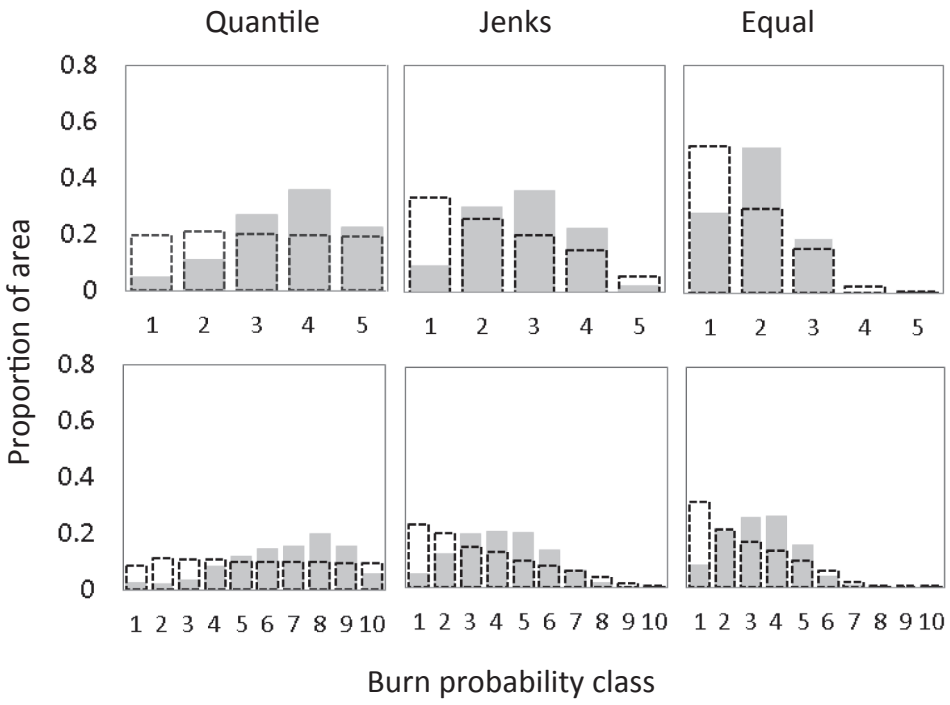

Fig. 6. Burned area proportions (solid shaded bars) versus study area null model proportions (hollow dashed bars) by burn probability class (1 = low, 5 or 10 = high) for the WC study area comparing two choices of class (bin) numbers (5 and 10). Shown for three classification methods: quantile, Jenks natural breaks, and equal interval.

Table 6
Proportion of observed burned areas with burn probability values exceeding a given percentile threshold (i.e., 50, 75, 80) in comparison with the proportion exceeding these thresholds across the study area as a whole (i.e., the null model) for two extents: (A) all burned areas; and (B) a random sample covering 0.005 of the burned area excepting CLGY where a 0.015 proportion was sampled. Due to the presence of spatial autocorrelation in the data, tests for significant differences apply only to sampled locations.

	Percentile threshold				
	50	67	75	80	90
Null model (study area proportion)	0.50	0.33	0.25	0.20	0.10
Proportion of burned area					
(A) All burned areas					
WC	0.75	0.48	0.34	0.21	0.06
LLB	0.82	0.64	0.53	0.41	0.25
FTMC	0.80	0.48	0.33	0.22	0.07
CLGY	0.42	0.03	0.01	0.01	0.00
WW	0.39	0.08	0.04	0.03	0.02
(B) Sampled locations					
WC	0.72[a]	0.43[b]	0.32[c]	0.20	0.05
LLB	0.78[a]	0.64[a]	0.50[a]	0.39[a]	0.26[a]
FTMC	0.70[a]	0.51[a]	0.36[a]	0.24[a]	0.07
CLGY	0.00	0.00	0.00	0.00	0.00
WW	0.31	0.08	0.04	0.02	0.02

[a] Significantly greater than the null proportion (Chi-squared, $p < 0.0001$).
[b] Significantly greater than the null proportion (Chi-squared, $p < 0.01$).
[c] Significantly greater than the null proportion (Chi-squared, $p < 0.05$).

probability map based on a 50th percentile performance expectation generates a uniform zone of relatively 'high' fire likelihood that spans half the study area (i.e., 529 490 ha to over 2.7 million hectares), which is not helpful for prioritizing fine-scale activities.

Map symbology had a profound impact on the appearance of our burn probability maps and corresponding assessment of map accuracy. Compared with Jenks natural breaks, equal intervals, or defined intervals, a quantile classification was the only method that resulted in burned areas falling preferentially in locations mapped in the highest burn probability classes. In our study areas, burn probability maps were generally effective when up to three quantile classes (bins) were used to summarize and visualize burn probability values. In determining whether or not to invest in a time- and computationally-intensive burn probability modeling exercise, prospective users of these maps should consider whether or not a fire likelihood map with just three zones (low, moderate, and high) each covering one-third of their study area is useful for informing their decisions.

We are aware of one prior study (Paz et al., 2011) that examined the performance of simulated burn probability values in relation to subsequent burned areas, in that case a single large fire. Our investigation of correspondence between 138 fires that burned 543 049 ha across five study areas and pre-fire assessments of burn probabilities provides new insight about the limitations of burn probability assessments in areas of low fire likelihood. The consistent negative relationship that we found between map accuracy and spatial precision for WC, LLB and FTMC study areas suggests burn probability maps may not be useful for informing fine-scale activities in these landscapes. Use of these maps for identifying firefighter safety zones or other fine-scale features relevant to public safety and community protection planning should be approached with extreme caution.

The early promise of burn probability simulation and widespread promotion of the method as an informative tool for mapping fire risk (i.e., Carmel et al., 2009; Keane et al., 2010; Weise et al., 2010; Finney et al., 2011; Parisien et al., 2013) occurred prior to any systematic effort to evaluate the effectiveness of the maps for applied decision support. Public distribution of free Burn-P3 software in Canada soon after its development enabled quick uptake of burn probability modeling by fire management agencies eager to adopt an evidence-based approach to operational fire risk mapping and mitigation planning. Burn-P3 has also been embraced by researchers who have incorporated model outputs

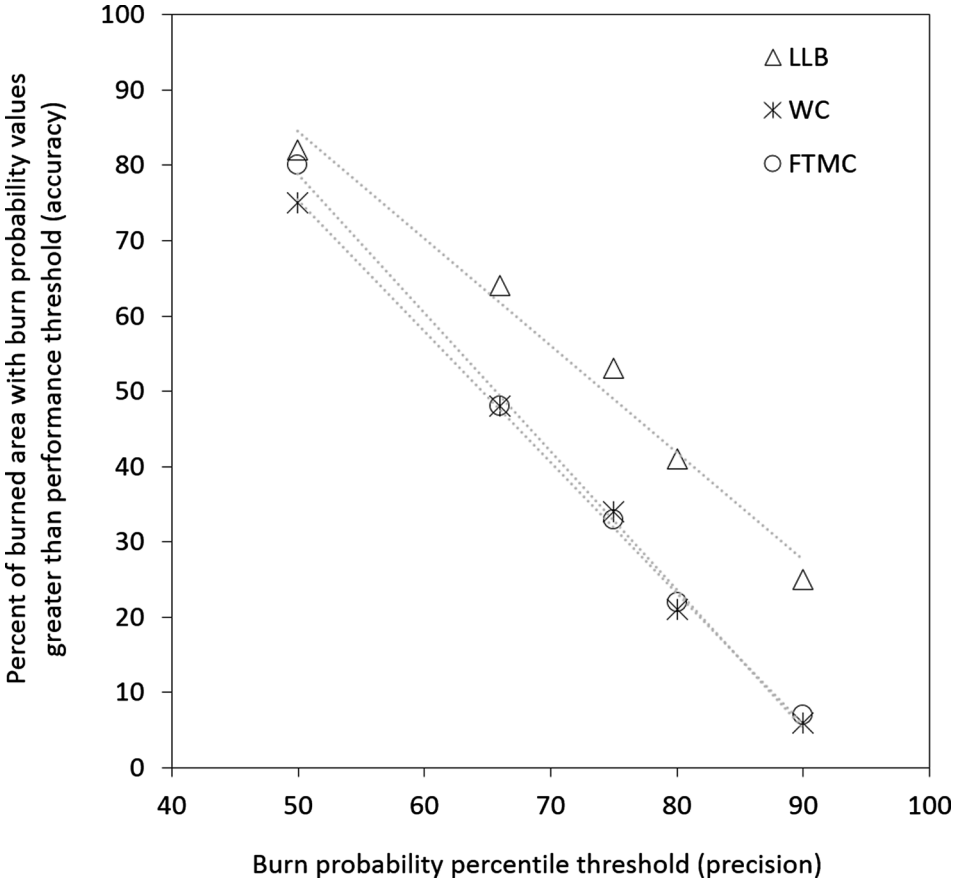

Fig. 7. Tradeoff between precision and accuracy when interpreting burn probability maps for three study areas (WC, LLB, FTMC). Symbols indicate performance threshold (percentile) and corresponding accuracy, defined as the proportion of observed burned areas associated with burn probability values above the threshold. For example, 75–80% percent of burned areas occurred in locations with burn probability values above the median (50th percentile threshold). Dotted lines denote linear trend by study area.

into investigations of a wide range of diverse topics such as conservation planning (Whitman et al., 2017; Stockdale et al., 2019), climate change impact assessment (Williamson et al., 2008; Wang et al., 2016), and risk-based decision making (Sherry et al., 2019). Our results suggest the merits of burn probability mapping for guiding applied management decisions warrants further evaluation and the use of these maps for research or other applications should be approached with caution and consideration of their shortcomings and apparent limitations.

We provide an assessment of the performance of burn probability maps in relation to expectations about what these maps communicate to decision makers. This differs from the standard validation processes that is always used to ensure Burn-P3 is properly parameterized to simulate fire processes representative of real world fire activity in the study area. In our study areas, historical fire records and burn probability simulations indicated the likelihood of burning is very low everywhere and the difference in likelihood between the lowest and highest burn probability values was notably small. In these low fire likelihood landscapes, it is not surprising that burned areas observed over the short term were at best generally consistent with burn probability patterns generated from tens of thousands of individual fire growth simulations representing thousands of possible variants of a single fire season.

Implications of our results are limited to the fire regime and fire environment conditions represented in our five Alberta study areas and to burn probability maps produced with the Burn-P3 simulation model. It is possible that burn probability maps produced by similar Monte Carlo methods using alternate software and conducted for study areas in other geographic locations may not exhibit the same limitations that we observed in our study areas.

Results of this study could be used to inform new approaches to fire risk mapping in northern forest ecosystems. In these ecosystems, fire regimes operate over large areas and long time periods. Characteristically large and infrequent fires typical of these ecosystems necessitate investigation of vast landscape areas and extended time periods to parameterize ignition processes and fire sizes to ensure simulated fires, generated by models like Burn-P3, are realistic. The usefulness of using a computationally intensive fine-scale fire spread model (i.e., Prometheus) imbedded within Burn-P3 to simulate detailed growth of tens of thousands of individual fires that occur over short time periods (minutes to days) in order to reveal broad-scale fire likelihood patterns merits further evaluation and exploration of alternative possible assessment methods. Approximating fire likelihood maps with readily known and easily mapped fire environment and fire regime factors known to influence burn probability values, such as the proximity of conifer fuels (Beverly et al., 2009), in combination with other thematic overlays could potentially offer a more efficient alternative to maps generated with Monte Carlo simulations in these landscapes and will require further investigation.

Declaration of Competing Interest

None

Appendix. – Burn probability class break values by study area and classification method

WC					CLGY				
Class	Quantile	Jenks	Equal	Defined	Class	Quantile	Jenks	Equal	Defined
1	0.0005	0.0009	0.0016	0.0027	1	0.0001	0.0002	0.0004	0.0007
2	0.0011	0.0019	0.0031	0.0053	2	0.0002	0.0004	0.0008	0.0013
3	0.0020	0.0030	0.0047	0.0074	3	0.0003	0.0007	0.0012	0.0018
4	0.0031	0.0042	0.0063	0.0077	4	0.0006	0.0010	0.0015	0.0019
5	0.0078	0.0078	0.0078	0.0078	5	0.0019	0.0019	0.0019	0.0019
LLB					**WW**				
Class	Quantile	Jenks	Equal	Defined	Class	Quantile	Jenks	Equal	Defined
1	0.0001	0.0004	0.0008	0.0014	1	0.0001	0.0002	0.0004	0.0006
2	0.0004	0.0009	0.0016	0.0028	2	0.0002	0.0004	0.0007	0.0012
3	0.0008	0.0015	0.0025	0.0039	3	0.0003	0.0007	0.0011	0.0017
4	0.0014	0.0022	0.0033	0.0041	4	0.0006	0.0010	0.0014	0.0018
5	0.0041	0.0041	0.0041	0.0041	5	0.0018	0.0018	0.0018	0.0018
FTMC									
Class	Quantile	Jenks	Equal	Defined					
1	0.0000	0.0063	0.0123	0.0209					
2	0.0126	0.0167	0.0246	0.0419					
3	0.0227	0.0271	0.0370	0.0585					
4	0.0319	0.0379	0.0493	0.0610					
5	0.0616	0.0616	0.0616	0.0616					

References

Alcasena, F.J., Salis, M., Ager, A., Castell, R.J., Vega-García, C., 2017. Assessing wildland fire risk transmission to communities in northern Spain. Forests 8, 30.

Beverly, J.L., Herd, E.P.K., Conner, J.C.R., 2009. Modeling fire susceptibility in west central Alberta, Canada. Forest Ecol. Manage. 258, 1465–1478.

Boisvert, R.F., Cools, R., Einarsson, B., 2005. Assessment of Accuracy and Reliability. In: Einarsson, B. (Ed.), Accuracy and Reliability in Scientific Computing. United States of America: Society for Industrial and Applied Mathematics (SIAM).

Carmel, Y., Paz, S., Johashan, F., Shoshany, M., 2009. Assessing fire risk using Monte Carlo simulations of fire spread. Forest Ecol. Manage. 257, 370–377.

Chiono, L.A., Fry, D.L., Collins, B.M., Chatfield, A.H., Stephens, S.L., 2017. Landscape-scale fuel treatment and wildfire impacts on carbon stocks and fire hazard in California spotted owl habitat. Ecosphere 8 (1), e01648.

Clarke, K.C., Brass, J.A., Riggan, P.J., 1994. A cellular automaton model of wildfire propagation and extinction. Photogramm. Eng. Remote Sens. 60, 1355–1367.

Farris, C., Pezeshki, C., Neuenschwander, L.F., 2000. A comparison of fire probability maps derived from GIS modelling and direct simulation techniques. In: Neuenschwander, L.F., Ryan, K.C. (Eds.), Crossing the millenium: integrating spatial technologies and ecological principles for a new age in fire management. Proceedings of the Joint Fire Science Conference and Workshop, Boise, Idaho, pp. 131–138 June 15–17, 1999.

Finney, M.A., 2004. FARSITE: fire area simulator – model development and evaluation, United States department of agriculture fire service. Rocky Mountain Res. Station Res. Paper RMRS-RP-4.

Finney, M.A., McHugh, C.W., Grenfell, I.C., Riley, K.L., Short, K.C., 2011. A simulation of probabilistic wildfire risk components for the continental United States. Stoch. Env. Res. Risk Assess. 25, 73–1000.

Forestry Canada Fire Danger Group, 1992. Development and structure of the Canadian Forest Fire Behavior Prediction System, Forestry Canada, Information Report ST-X-3, 63 p.

Jenks, G.F., 1967. The data model concept in statistical mapping. Int. Yearbook Cartography 7, 186–190.

Keane, R.E., Drury, S.A., Karau, E.C., Hessburg, P.F., Reynolds, K.M., 2010. A method for mapping fire hazard and risk across multiple scales and its application in fire management. Ecol. Model. 221, 2–18.

Lautenberger, C., 2017. Mapping areas at elevated risk of large-scale structure loss using Monte Carlo simulation and wildland fire modeling. Fire Saf. J. 91, 768–775.

Lozano, O.M., Salis, M., Ager, A.A., Arca, B., Alcasena, F.J., Monteiro, A.T., Finney, M.A., Del Giudice, L., Scoccimarro, E., Spano, D., 2017. Assessing climate change impacts on wildfire exposure in Mediterranean areas. Risk Anal. 37, 1898–1916.

Mallinis, G., Mitsopoulos, I., Beltran, E., Goldammer, J., 2016. Assessing wildfire risk in cultural heritage properties using high spatial and temporal resolution satellite imagery and spatially explicit fire simulations: the case of Holy Mount Athos. Greece. Forests 7, 46.

Natural Regions Committee, 2006. Natural Regions and Subregions. In: Compilers. Government of Alberta Publ. T/852, Edmonton, AB, Canada.

Nobert, S., Krieger, K., Pappenberger, F., 2015. Understanding the roles of modernity, science, and risk in shaping flood management. Wiley Interdisciplin. Rev. Water 2, 245–258.

Parisien, M.A., Kafka, V.G., Hirsch, K.G., Todd, J.B., Lavoie, S.G., Maczek, P.D., 2005. Mapping wildfire susceptibility with the Burn-P3 simulation model. Canadian Forest Service. Northern Forestry Centre Information Report NOR-X-405.

Parisien, M.A., Walker, G.R., Little, J.M., Simpson, B.N., Wang, X., Perrakis, D.D.B., 2013. Considerations for modeling burn probability across landscapes with steep environmental gradients: an example from the Columbia Mountains, Canada. Nat. Hazards 66, 439–462.

Paz, S., Carmel, Y., Jahshan, F., Shoshany, M., 2011. Post-fire analysis of pre-fire mapping of fire-risk: a recent case study from Mt. Carmel (Israel). For. Ecol. Manage. 262, 1184–1188.

Salis, M., Laconi, M., Ager, A.A., Alcasena, F.J., Arca, B., Lozano, O.M., Oliveira, A.S., Spano, D., 2016. Evaluating alternative fuel treatment strategies to reduce wildfire losses in a Mediterranean area. For. Ecol. Manag. 368, 207–221.

Salis, M., Del Giudice, L., Arca, B., Ager, A.A., Alcasena-Urdiroz, F., Lozano, O., Bacciu, V., Spano, D., Duce, P., 2018. Modeling the effects of different fuel treatment mosaics on wildfire spread and behavior in a Mediterranean agro-pastoral area. J. Environ. Manage. 212, 490–505.

Seipel, S., Lim, N.J., 2017. Color map design for visualization in flood risk assessment. Int. J. Geographical Informat. Sci. 31, 2286–2309.

Sherry, J., Neale, T., McGee, T.K., Sharpe, M., 2019. Rethinking the maps: a case study of knowledge incorporation in Canadian wildfire risk management and planning. J. Environ. Manage. 234, 494–502.

Stockdale, C., Barber, Q., Saxena, A., Parisien, M.A., 2019. Examining management scenarios to mitigate wildfire hazard to caribou conservation projects using burn probability modelling. J. Environ. Manage. 233, 238–248.

Tymstra, C., Bryce, R.W., Wotton, B.M., Tayalor, S.W., Armitage, O.B., 2010. Development and structure of prometheus: the Canadian Wildland fire growth simulation model. Nat. Resour. Can., Can. For. Serv., North. For. Cent., Edmonton, AB. Inf. Rep. 88 NOR-X-417.

Van Wagner, C.E., 1987. Development and structure of the Canadian Forest Fire Weather Index System. Canadian Forest Service. Forestry Technology Report 25.

Wang, X., Parisien, M.-A., Taylor, S.W., Perakis, D.D., Little, J.M., Flannigan, M.D., 2016. Future burn probability in south-central British Columbia. Int. J. Wildland Fire 25, 200–212.

Weise, D.R., Stephens, S.L., Fujioka, D.M., Moody, T.J., Benoit, J., 2010. Estination of fire danger in Hawai'i using limited weather data and simulation. Pac. Sci. 64, 199–220.

Whitman, E., Parisien, M.-A., Price, D.T., St-Laurent, M.-H., Johnson, C.J., DeLancey, E.R., Arseneault, D., Flannigan, M.D., 2017. A framework for modeling habitat quality in disturbance-prone areas demonstrated with woodland caribou and wildfire. Ecosphere 8, e01787.

Woo, H., Chung, W., Graham, J.M., Lee, B., 2017. Forest fire risk assessment using point process modelling of fire occurrence and Monte Carlo fire simulation. Int. J. Wildland Fire 26, 789–805.

Ye, T., Wang, Y., Guo, Z., Li, Y., 2017. Factor contribution to fire occurrence, size, and burn probability in a subtropical coniferous forest in East China. PLoS ONE 12, e0172110.

Williamson, T.B., Price, D.T., Beverly, J., Bothwell, P.M., Frenkel, B., Park, J., Patriquin, M.N., 2008. Assessing potential biophysical and socioeconomic impacts of climate change on forest-based communities: a methodological case study. Natural Resources Canada, Canadian Forest Service, Northern Forestry Centre, Edmonton, Alberta. Information Report NOR-X-415E. 136 p.